WELDING RESEARCH

SUPPLEMENT TO THE *WELDING JOURNAL*, MAY 1997
Sponsored by the American Welding Society and the Welding Research Council

RESEARCH/DEVELOPMENT/RESEARCH/DEVELOPMENT/RESEARCH/DEVELOPMENT/RESEARCH/DEVELOPMENT

Influence of Mn and Ni on the Microstructure and Toughness of C-Mn-Ni Weld Metals

Increasing the manganese and nickel levels changes the weld metal microstructure by promoting acicular ferrite at the expense of proeutectoid ferrite

BY Z. ZHANG and R. A. FARRAR

Abstract. A systematic investigation has been carried out to study the microstructure and toughness of C-Mn-Ni low-alloy shielded metal arc (SMA) weld metals. The manganese and nickel concentrations were progressively changed to determine their influence on weld microstructure and mechanical properties as well as to identify their interactions. The results obtained showed that manganese and nickel have considerable effect on the weld metal microstructure, and both Mn and Ni affect the microstructure in a similar way, *i.e.*, promoting acicular ferrite at the expense of proeutectoid ferrite (grain boundary ferrite and ferrite sideplates). The results in the top bead also showed that there is an optimum composition range that produces an optimum balance of weld metal microstructures. For optimum toughness, a combination of 0.6–1.4% manganese and 1.0–3.7% nickel is suggested. Additions beyond this limit promotes the formation of martensite and other microstructural features, which may be detrimental to weld metal toughness.

Introduction

Over the past few years, more and more critical service conditions in welded structures, such as offshore platforms, cryogenic plants and associated pipework construction, have increased demands for alloy steel weld metals with improved mechanical properties, especially low-temperature toughness. The requirements for excellent toughness have promoted a continuous development of advanced welding consumables capable of producing weld metals with optimum microstructure and mechanical properties.

From the large number of investigations dealing with low-carbon low-alloy weld metals, the as-deposited microstructure is commonly described as consisting of the following major microstructural components: grain boundary ferrite (PF(G)), ferrite sideplates (or Widmanstätten sideplates) (FS(A)), acicular ferrite (AF) and, in certain circumstances, martensite (M). It is generally believed that a microstructure that contains a high proportion of acicular ferrite displays optimum weld metal strength and toughness properties. This is attributed to its small grain size (typically 1–3 μm), in which each lath is separated by high angle grain boundaries. On the other hand, the formation of a large proportion of grain boundary ferrite, ferrite sideplates, or martensite, has been found to be detrimental to toughness, because these structures provide preferential easy crack propagation paths, which offer a low resistance during the weld metal cleavage fracture (Refs. 1–3).

There have been some systematic investigations into C-Mn-Ni low-alloy weld metals. These include studies on the microstructure and mechanical properties of as-deposited welds carried out by Taylor and Evans (Ref. 4) and Evans (Ref. 5), and the continuous cooling transformation kinetics of the C-Mn-Ni weld metals conducted by Harrison and Farrar (Refs. 6, 7) and the current authors (Refs. 8, 9). These previous studies paid primary attention to microstructural features of C-Mn-Ni welds and how these are influenced by different additions of nickel, and how the weld metal toughness changed with variations in the nickel and manganese contents (Refs. 4, 5). In the investigation of kinetics, using continuous cooling transformation diagrams (CCT), the microstructural development in C-Mn-Ni weld metals was studied, and different factors that influ-

KEY WORDS

C-Mn-Ni Weld Metal
Microstructure
Acicular Ferrite
Toughness
Composition Balancing

ZHUYAO ZHANG and R. A. FARRAR are with the Department of Mechanical Engineering, University of Southampton, Southampton, U.K.

Table 1 — Chemical Composition of the Core Wire (wt-%)

Wire	C	Mn	Si	S	P	Ni	Cr	Mo	Cu	Al+Ti	N (ppm)
MS1	0.01	0.10	0.02	<0.015	<0.012	<0.06	<0.06	<0.06	<0.06	<0.4	<50

Table 2 — The Chemical Composition of the Weld Metals (wt-%)

Weld Code	AWS Specification	C	Mn(a)	Si	S	P	Ni(a)	Ti	Mo	Al	Cu	O	N
A0	A5.5/E7018-G	0.042	1.57	0.46	0.010	0.013	0.03	0.016	0.007	0.004	0.050	nd(c)	nd
A1	A5.5/E8016-G	0.048	1.68	0.50	0.011	0.015	0.95	0.019	0.010	0.007	0.050	0.0254	0.0134
A2	A5.5/E8016-C1	0.041	1.67	0.49	0.009	0.013	2.48	0.018	0.008	0.005	0.056	nd	nd
B1	A5.5/E8018-C1	0.037	0.85	0.50	0.008	0.013	2.56	0.021	0.008	0.005	0.060	0.0310	0.0100
82	A5.5/E8016-C2	0.057	0.67	0.53	0.008	0.013	3.32	0.024	0.008	0.006	0.064	nd	nd
B3	EC	0.048	0.78	0.66	0.008	0.015	5.53	0.025	0.010	0.007	0.074	nd	nd
C1	EC(b)	0.034	0.36	0.55	0.013	0.008	5.58	0.023	0.008	0.006	0.078	nd	nd

(a) Design changes.
(b) EC = experimental consumables.
(c) nd = not determined.

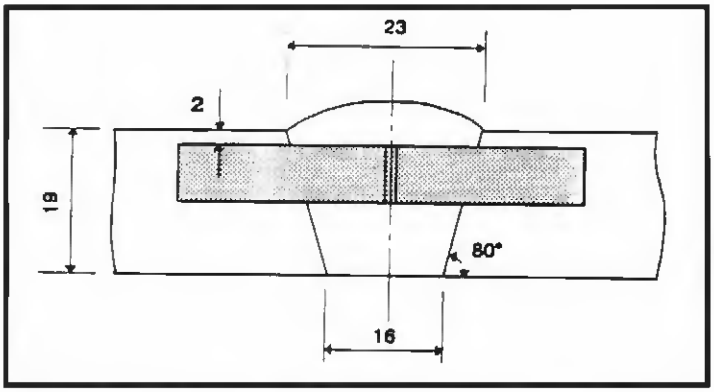

Fig. 1 — Schematic diagram showing joint geometry and location of Charpy specimens (dimensions in mm).

ence this behavior were demonstrated (Refs. 6–9). There have been some other less systematic compositional works that studied C-Mn-Ni welds. For instance, Abson (Ref. 10) recently carried out investigations on as-welded toughness of gas-shielded C-Mn-Ni deposits containing 1.0% nickel with different types of welding wires, while Surian, *et al.* (Ref. 11), studied shielded metal arc C-Mn-Ni welds with 3% nickel to demonstrate the effect of oxygen content on the toughness of these welds.

Despite the level of research efforts directed toward C-Mn-Ni weld metals, the factors controlling strength and toughness are not fully understood. These include a) how a wider range of nickel and manganese contents influence the weld metal microstructure and the resultant mechanical properties; b) the interaction between manganese and nickel and the correlation with an optimum microstructure, and therefore, optimum toughness; and c) the effect of additions of manganese and nickel on the morphologies of the microstructural components and other microstructural features, and how this can be related to weld metal toughness. The present work addresses these factors.

Experimental Details

Electrodes

A series of C-Mn-Ni iron powder, low-hydrogen basic electrodes, coded A(0-2), B(1-3) and C(1), were prepared using 4.0-mm size consumahles. The coating ratio of the electrodes was ~1.5. Different amounts of alloying powder were added to the coatings to produce comparable levels of manganese and nickel in all weld metal samples, nominally 0.3, 0.7 and 1.6% Mn and 0, 1.0, 2.5, 3.5 and 5.5% Ni. The core wire used was MS1. Its chemical composition is listed in Tahle 1. The electrodes were baked at 300°C for 2 h.

Weld Compositions

A series of shielded metal arc C-Mn-Ni weld metals was used. Three levels of manganese content, namely 0.3%, 0.7% and 1.6%, were designed to balance with different nickel content ranges, *i.e.*, 0–2.5%, 2.5–5.5% and 5.5%, respectively. The microstructures formed in the as-deposited regions and reheated regions were examined, and correlated with the mechanical properties, particularly toughness. The results were compared with existing data produced by other authors.

Weld Preparation

The welding was carried out on B5970-070M20[1] plate with a nominal chemical composition of 0.25% (max.) C, 1.0% Mn, 0.06% S and 0.06% P. The thickness of the plate was 19 mm. The joint geometry is illustrated in Fig. 1. Alternating current was employed. The process conditions were current: 145 A, voltage: 18 V, average travel speed: 2.42 mm/s^{-1} and a nominal heat input of 1.2 kJ/mm^{-1}. The interpass temperature was held at 150°C. Using three beads per layer (two beads for the first layer), the total number of runs was 23. The welding was done in the downhand position.

Chemical Composition Analysis and Metallography

The chemical compositions of the as-deposited weld metals were determined by a Bausch & Lomb ARL-3560 optical emission spectrometer using samples

1. *Equivalent to AISI-SAE1022.*

2. Guide to Light Microscopy Examination of Ferritic Weld Metals, *IIW Doc. No. IX-1533-88, June 1988.*

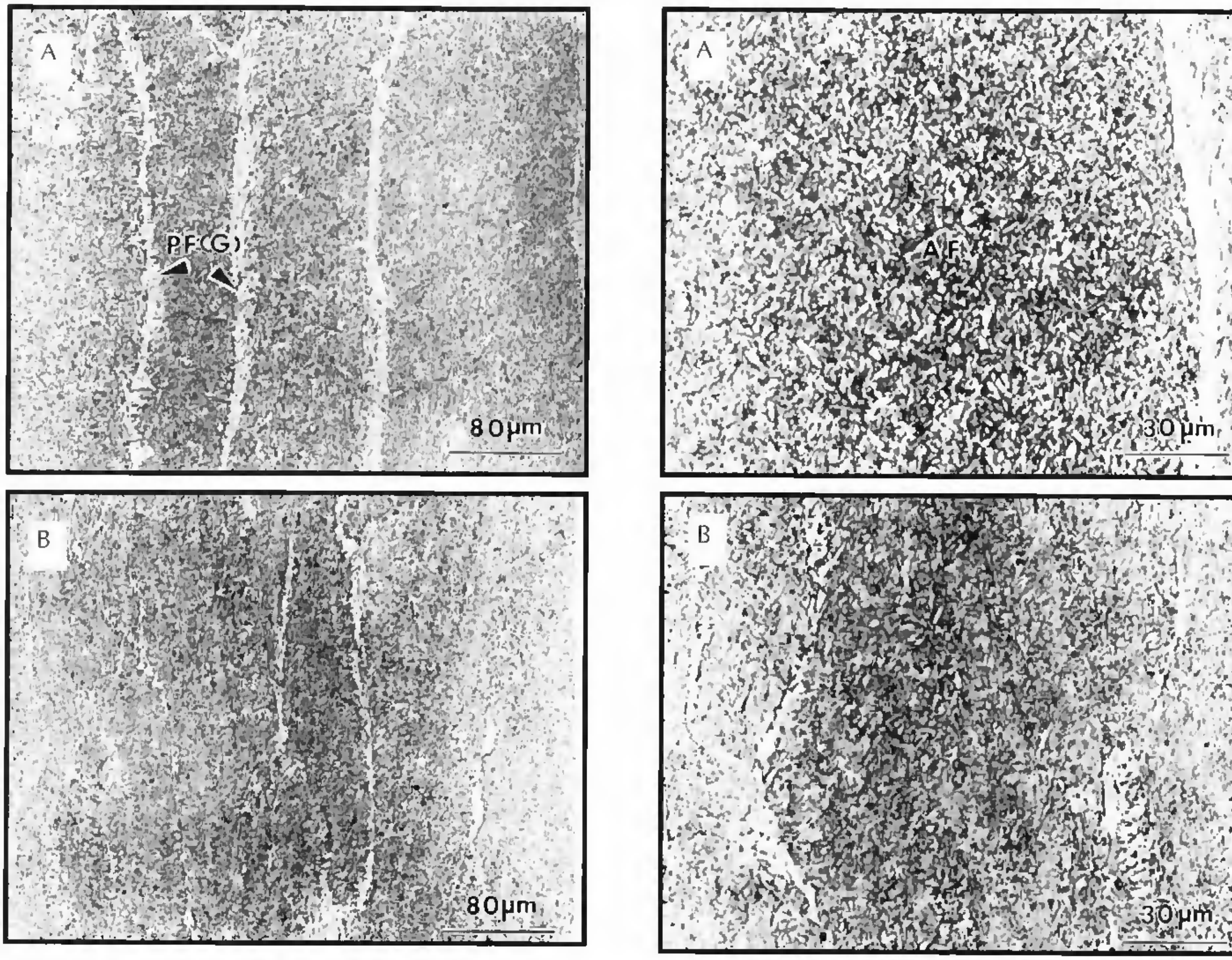

Fig. 2 — Microstructure of the as-deposited top bead welds (1.6% Mn). A — A1 weld (1.0% Ni); B — A2 weld (2.5% Ni).

containing the full section of the weld (the actual target size was 16 mm in diameter) and checked by Quantovac methods. The oxygen and nitrogen contents of some welds (A1 and B1) were assessed by a Leco TC-136 machine.

All metallographic specimens from each weld were prepared by standard metallographic methods. The polished samples were etched in 2% Nital. Optical examination was carried out on a Neophot II microscope. A JEOL JSM-T300 scanning electron microscope (SEM) was employed to assess the detailed morphology of the acicular ferrite produced.

Quantitative metallography using the standard Welding Institute method[2] was used to assess the proportions of the different microstructural constituents in the as-deposited weld metal and to measure the prior austenite grain size. The prior austenite grain size was determined using the linear intercept method (Ref. 12) and the grain size (*i.e.*, the columnar grain width) was measured using the grain boundary ferrite veins. The quantitative measurement of the volume fractions of the various microconstituents was carried out by employing a point counting method; this used a 7 x 7 grid comprised of 1-cm squares (*i.e.*, 49 counting points for one field) placed on the microscope projection screen at a magnification of 500. Forty fields were examined, which resulted in 1960 points being counted for each individual specimen. The areas used for the quantification of microstructures of as-deposited top bead welds were chosen following the suggestion of Davey and Widgery (Ref. 13).

Mechanical Examinations

<u>Charpy Impact Test</u>

Charpy V-notch specimens (10 x 10 x 55 mm) were extracted from the welds in the manner shown in Fig. 1. A through-thickness notch was machined parallel to the centerline of the welds. To ensure the notch was located in the center of the weld beads, 4% Nital was used to outline the welds in the Charpy specimens. The notch size of every Charpy specimen was carefully checked before testing. The impact tests were carried out at eight different temperatures between 20° and −80°C, to obtain full transition curves.

SEM was used to examine the fracture surfaces to establish the failure mode of the different weld metals.

<u>Hardness Test</u>

Vickers hardness tests using a 10-kg load were conducted on a full macrosection of each of the weld metals across the centerline of the welds. The space between two adjacent testing spots was 1 mm.

Results

Chemical Analysis Results

The chemical compositions of the weld metals are listed in Table 2. From the table, it can be seen that the yields of

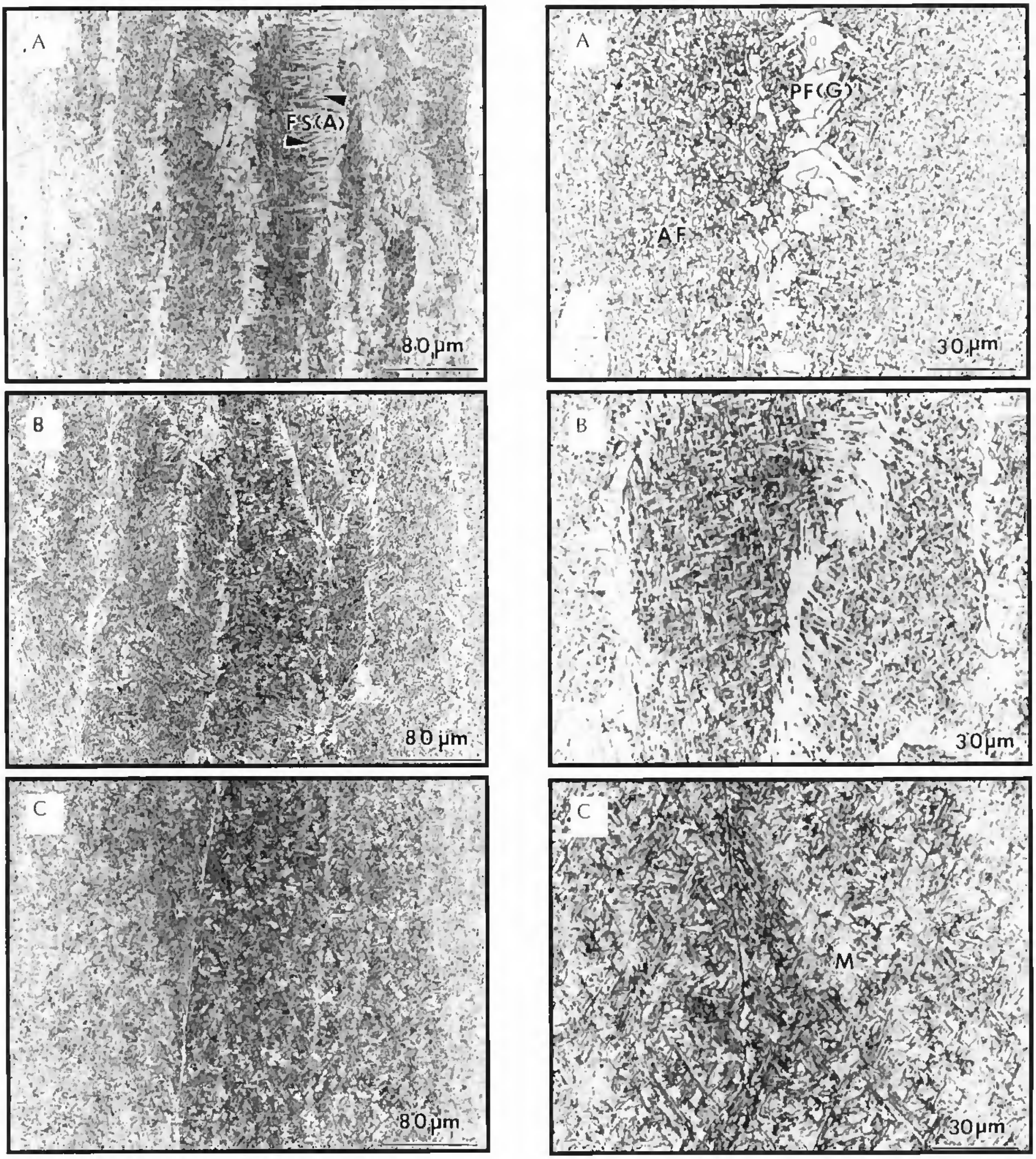

Fig. 3 — Microstructure of the as-deposited top bead welds (0.7% Mn). A — B1 weld (2.5% Ni); B — B2 weld (3.5% Ni); C — B3 weld (5.5% Ni).

nickel, manganese and other elements were as expected, the exceptions being the B2 weld, which had a slightly lower nickel level, and the B1 weld, which had a higher manganese content. The carbon contents were essentially within the target range, namely 0.04–0.05%, although B2 contained slightly higher carbon. The carbon content drift was generally within 0.015%. Nevertheless, these small variations in chemical composition were not considered to be significant compared with the design changes in nickel and manganese concentrations.

The oxygen levels of the weld metals were examined using two of the welds (A1 and B1), which represented either high (1.6%) or intermediate (0.7%) manganese level welds. The analyses showed that the oxygen contents of these welds were within the predicted oxygen level regime, typically 250–350 ppm. In the case of the other welds, as there were no obvious differences in the main deoxi-

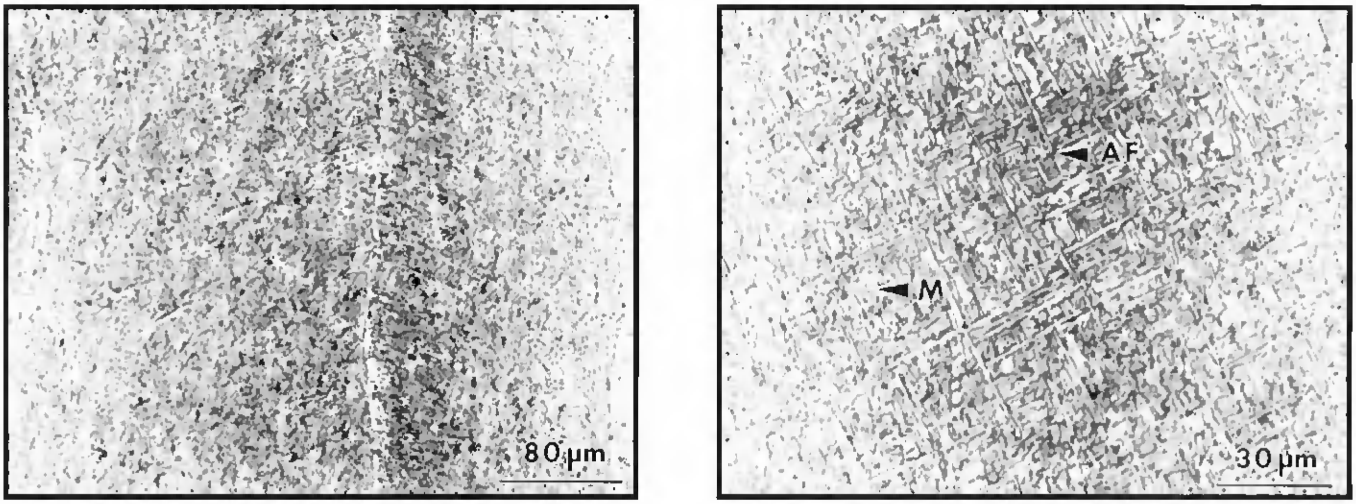

Fig. 4 — Microstructure of the as-deposited top bead weld (C1: 0.3% Mn, 5.5% Ni).

dants (such as silicon), and as the welds were produced by the same welder using the same procedure, the oxygen levels were assumed to range between 250 and 350 ppm.

Microstructure of the Weld Metals

Microstructure of the As-Deposited Top Beads

The microstructures of the as-deposited weld metals (top beads) with different manganese levels are shown in Figs. 2–4. The volume fraction of different microconstituents and the average columnar (austenite) grain width are listed in Table 3. The microstructure of these weld metals consists mainly of acicular ferrite, grain boundary ferrite, ferrite sideplates, and in some circumstances, martensite. Typical examples of these phases are illustrated in Figs. 2–4.

The results of the optical examinations and the data listed in Table 3 indicate the significant influence of manganese and nickel on the microstructure of the weld metals. At a higher manganese level (*i.e.*, 1.6% Mn), when the nickel content was increased from 0 to 1.0%, the acicular ferrite content increased considerably while grain boundary ferrite decreased, and the microstructure became dominated by acicular ferrite; when the nickel content was increased to 2.5%, about 6% martensite appeared in the microstructure associated with a further reduction in grain boundary ferrite. In general, with the addition of nickel, the volume fraction of acicular ferrite structure increased at the expense of grain boundary ferrite. At higher nickel contents, the increase in acicular ferrite was accompanied by the presence of the martensitic structure, while grain boundary ferrite was obviously reduced and sideplate structures decreased slightly.

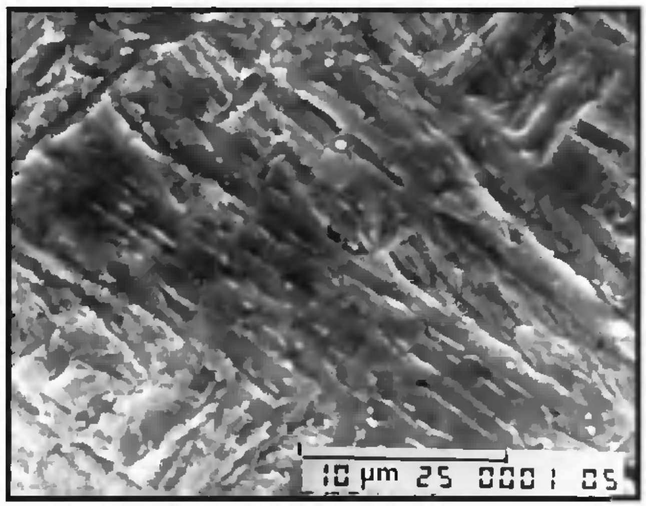

Fig. 5 — Morphology of martensite in high-nickel-content weld (C1 weld).

When the manganese level dropped to 0.7% and nickel was kept at an intermediate level (2.5%), grain boundary ferrite and ferrite sideplates initially increased and were accompanied by a decrease in acicular ferrite and elimination of martensite compared with the 1.6% Mn weld metal. Further additions of nickel, especially when nickel content was greater than 3.5%, resulted in a considerable reduction of grain boundary ferrite and ferrite sideplates, and increase of acicular ferrite. When the nickel content was increased to 5.5%, martensite in the weld reached ~30%, while grain boundary ferrite almost disappeared. However, by reducing manganese further to 0.3%, a slight decrease in martensite and increase in higher temperature transformation products was obtained as expected (Refs. 6–9). In the B3 and C1 welds, lath martensite was clearly present as indicated in both the optical (Figs. 3, 4) and the SEM photographs (Fig. 5).

With the addition of nickel, the

Table 3 — Results of Quantitative Metallography for the As-Deposited Weld Metal Microstructure

Weld Code	Microstructural constituents (%) PF(G)	FS(A)	AF	M	Average columnar width (µm)
A0	18	13	69		100
A1	11	12	77		110
A2	5	10	79	6	61
B1	21	22	57		69
B2	16	23	61		64
B3	1	6	63	30	215
C1	3	8	67	22	180

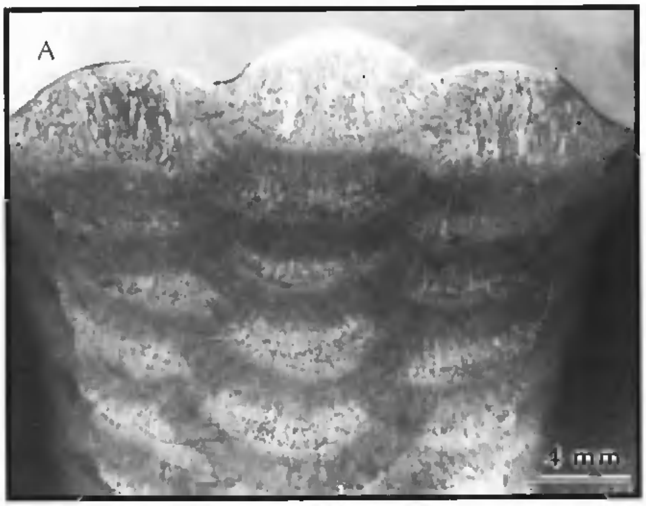

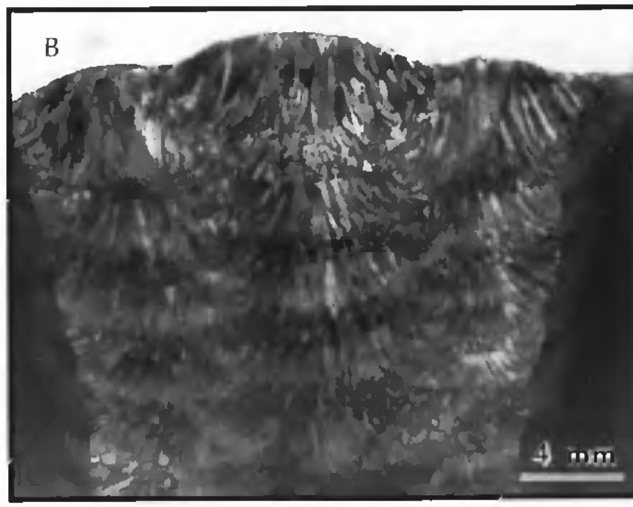

Fig. 6 — Effect of the nickel content on weld columnar structure. A — B1 weld (2.5% Ni); B — B3 weld (5.5% Ni).

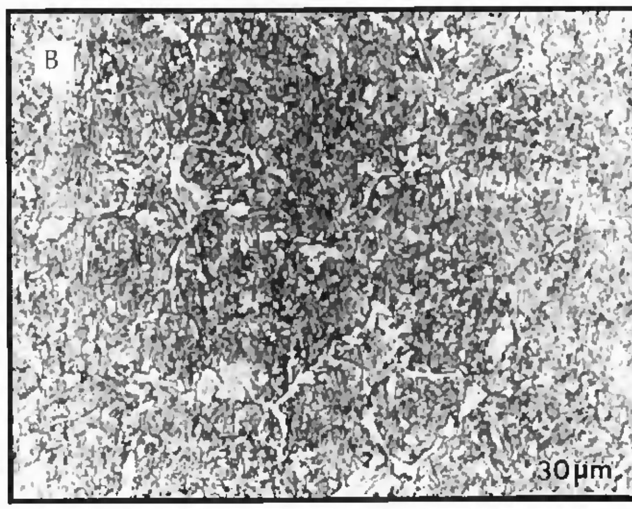

Fig. 7 — Microstructure of high-temperature reheated regions of A1 and A2 welds (1.6% Mn). A — A1 weld (1.0% Ni); B — A2 weld (2.5% Ni).

change in the columnar grain size (width) was very interesting. At the higher manganese content (~1.6%), increasing the nickel content depressed the prior austenite grain. When the nickel concentration changed from 0 to 2.5%, the average width of the columnar grains in the top beads was reduced by 39% (*i.e.*, from 100 to 61 μm). With a lower manganese level (0.7%), and 2.5 or 3.5% nickel content, the width of the austenite grains was still refined to less than 70 μm. But when the nickel content increased to 5.5%, the columnar size dramatically increased by more than three times to greater than 200 μm (Ref. 14). This is clearly illustrated in Figs. 3 and 4. Even under macro-observation, this grain coarsening effect can be clearly seen, as shown in Fig. 6, which demonstrates the macrostructure of the 0.7% Mn welds containing 2.5 and 5.5% nickel. With 2.5% Ni, the columnar structure was refined, but at high nickel contents (5.5%), it was coarsened and extremely coarse grains, "elephant structure," were produced. Comparing the data obtained, the effect of manganese on the columnar size is also obvious. The extent of its effect on the C-Mn-Ni welds depends synergistically on the nickel level. At the 2.5% Ni content, a reduction of 0.9% in manganese (from 1.6 to 0.7%) increased the grain size by 13%, while at a higher nickel concentration (5.5%), a drop of manganese from 0.7 to 0.3% resulted in a 16% depression of the grain width. A detailed discussion on the columnar grain growth in C-Mn-Ni weld metals and the effect of alloying elements is presented in a separate paper (Ref. 14).

In addition, detailed metallographic examination revealed that the aspect ratios and morphology of acicular ferrite obtained in the weld metals changed with chemical composition and with the nickel content in particular. When the nickel content was increased, the aspect ratio was increased, and the acicular ferrite laths became very thin and sharp. This change in acicularity of the acicular ferrite has been discussed in a recent paper (Ref. 15).

Reheated Weld Metals

In the series of weld metals used in this present study approximately 50% of the weld metal was reheated — Fig. 6. Optical examination of the high-temperature reheated regions, directly below the top beads in the welds, which had experienced high temperature (~1300°C) reheating during the thermal cycle of the subsequent weld beads, revealed a marked microstructural change as nickel was added — Figs. 7, 8. The effect was essentially the same as that in the as-deposited metals: the grain boundary ferrite and sideplates at the prior γ grain boundaries were progressively replaced by acicular ferrite (nickel content up to 3.5%), and even martensite (5.5% Ni).

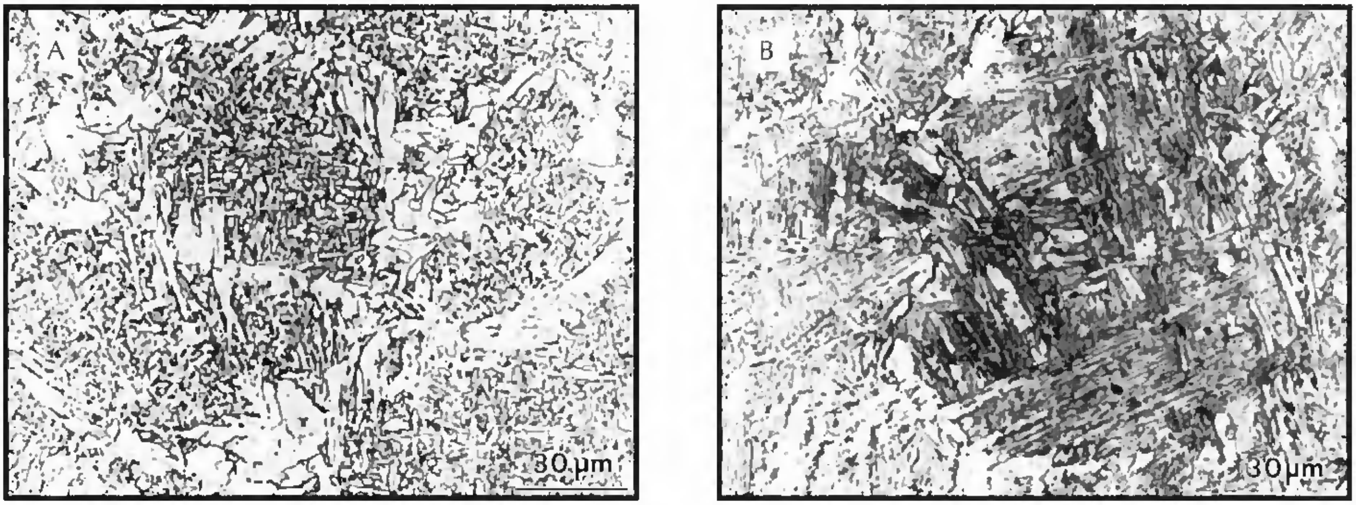

Fig. 8 — Microstructure of high-temperature reheated regions of the B1 and B3 weld (0.7% Mn). A — B1 weld (2.5% Ni); B — B3 weld (5.5%).

In the lower temperature (~900°C) reheated regions, the effect seemed more significant, as shown in Figs. 9 and 10. The structure with high Mn-low Ni and low Mn-medium Ni contents were refined as usual — Figs. 9A, 10A. With high Mn-medium Ni or low Mn-high Ni, the weld structures appeared to show distinctive "structure inheritance" features, indicating that at high levels of nickel, the normal changes in grain structure due to recrystallization did not remove the preexisting structure — Figs. 9B, 10B.

At the even lower temperature (<900°C) reheated regions, large additions of nickel (as in the A2, B3 and C1 welds) produced a considerable change in the microstructure; and a segregation structure was observed with the morphologies displaying either a network or parallel boundaries, as shown in Fig. 11. SEM energy dispersive X-ray analyses (EDS) carried out along a lateral section of the segregation structures indicated that the segregation sites were rich in nickel, manganese and silicon — Fig. 12. Studies (Refs. 8, 16) in parallel with the current work have revealed that the elemental segregation in the welds was a result of solidification rather than the product of the lower temperature transformations (*i.e.*, γ-α transformation). This resulted in a locally distributed martensitic structural banding saturated with nickel, manganese, silicon and, possibly, carbon. This martensitic structure would then decompose during the reheating at temperatures above 600°C, the product of the reaction then outlining the pattern of the segregation (Ref. 8). Further TEM work carried out by Zhang and Farrar (Ref. 16) identified the precipitated particles as a type of orthorhombic carbide (M_aC_b).

Hardness Results

Average hardness traverses along the through-thickness centerline of the welds containing both the as-deposited and reheated microstructures are plotted in Figs. 13 and 14 to illustrate the change of hardness with the variations in the manganese and nickel contents. These figures reveal that manganese and nickel have a powerful effect in increasing hardness of the deposits, manganese having a stronger effect than nickel. The major influence of these elements is through changes in microstructural constituents. In general, the trend is that, hardness of the weld metals rose with the amount of either acicular ferrite or martensite structure in the microstructure.

Impact Toughness Results

Average Charpy-V data are shown in Table 4. The impact transition curves of the weld metals obtained from the average of the scatter bands are plotted in Fig. 15A, B for the welds of 1.6% Mn or 0.7% Mn levels and in Fig. 16 for the welds of 5.5% Ni content, but with different manganese additions.

At the 1.6% manganese level, an addition of 1.0% nickel increased the toughness of the weld, *i.e.*, increased both upper shelf and lower shelf, hence reducing the transition temperature by about 5°C. When the nickel content was increased to 2.5%, however, the whole impact curve was depressed, which is not surprising as the yield strength would rise with increasing hardenability. With a lower manganese level (0.7%), the addition of a medium amount of nickel (2.5%) resulted in excellent toughness, but a slight decrease in the upper shelf. Increasing the nickel content to 3.5%, the properties were still satisfactory; however, the upper shelf was depressed further and there was indication that the

Table 4 — Results of Charpy V-Notch Impact Testing (Average of Three Specimens)

Weld	Average absorbed energy (J)							
Code	20°C	0°C	–20°C	–40°C	–50°C	–60°C	–70°C	–80°C
A0	206	168	158	126	92	42	21	nd[a]
A1	194	202	162	141	89	65	nd	40
A2	141	107	81	69	34	nd	25	nd
B1	203	174	164	153	127	77	nd	34
B2	174	169	155	124	118	76	52	38
B3	91	81	43	40	31	33	20	nd
C1	116	115	105	85	55	55	nd	33

(a) nd = not determined

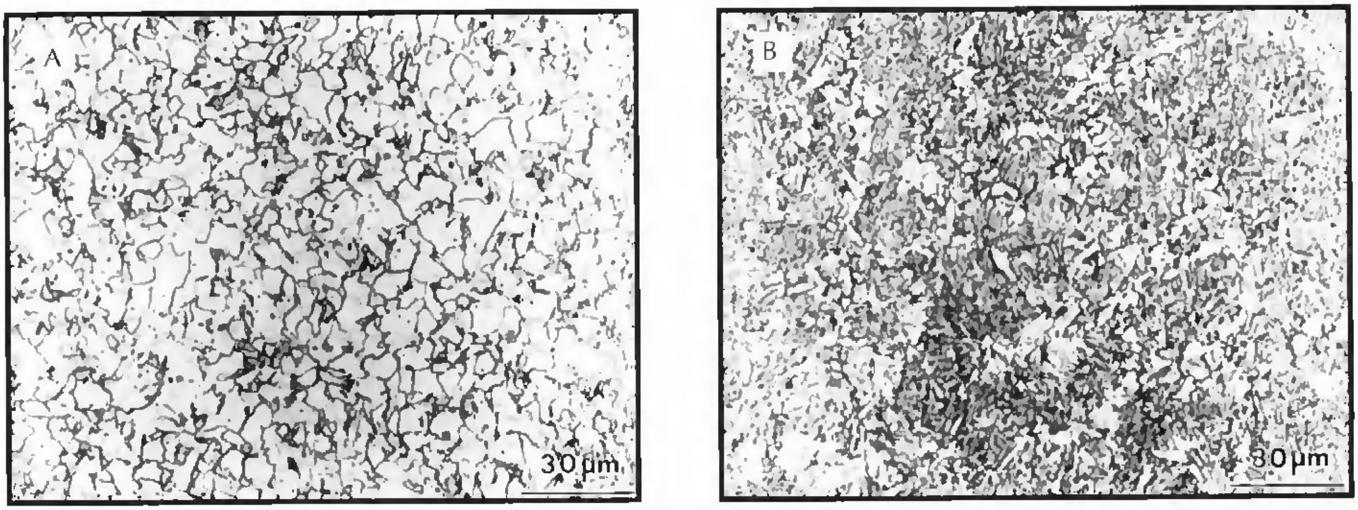

Fig. 9 — Microstructure of low-temperature reheated regions of the A1 and A2 welds (1.6% Mn). A — A1 weld (1.0% Ni); B — A2 weld (2.5% Ni).

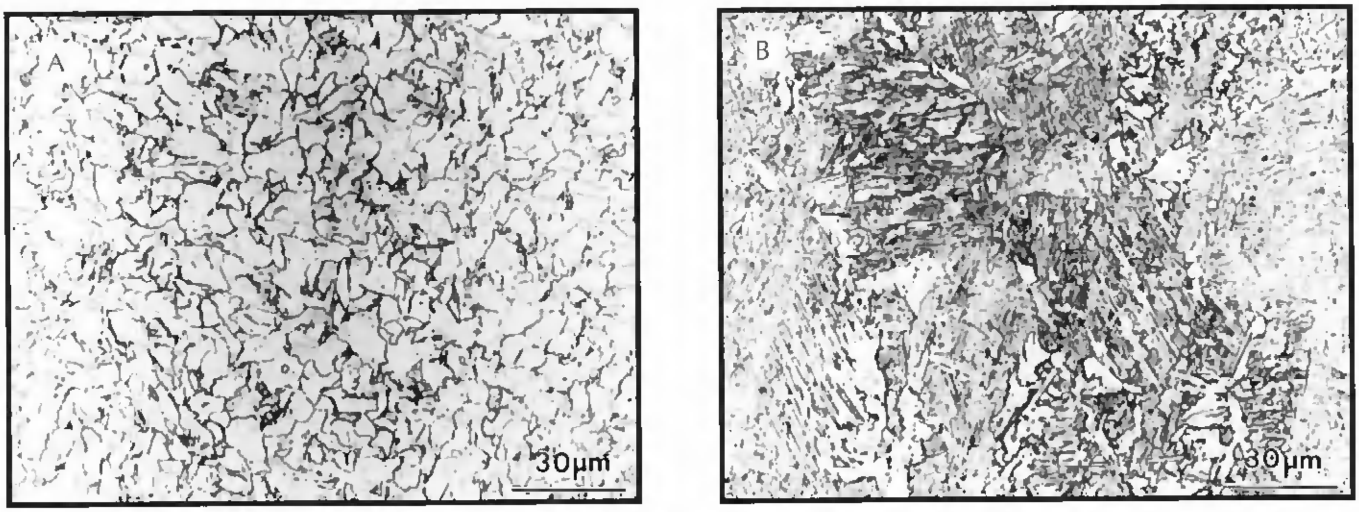

Fig. 10 — Microstructure of low-temperature reheated regions of the B1 and B3 welds (0.7% Mn). A — B1 weld (2.5% Ni); B — B3 weld (5.5% Ni).

toughness had begun to decrease. With a nickel content of 5.5%, the toughness dropped considerably. Reducing the manganese to 0.3%, the toughness was obviously improved, but because the basic structure was similar to that of the B3 weld, the toughness was still unsatisfactory.

Discussion

Influence of Manganese and Nickel on the As-Deposited Weld Metal Microstructure

The results of both metallographic observation and quantitative measurements indicated that the microstructure of the C-Mn-Ni weld metals consisted mainly of grain boundary ferrite, ferrite sideplates, acicular ferrite and, in some circumstances, martensitic structures. The volume fractions of these phases were, to very large extent, dependent upon the chemical composition of the welds, namely the nickel and manganese contents.

The results obtained show that, generally, the addition of nickel to weld metals effectively promotes the formation of acicular ferrite while significantly reducing the amount of grain boundary ferrite, both at the higher and lower manganese levels, in the as-deposited regions (Table 3). This confirms the previous results reported by Evans (Ref. 5). In the case of the sideplate structures, the effect of nickel varied with its concentration in combination with manganese, as summarized in Table 5. At the 1.6% Mn level, increasing nickel from 0 to 2.5% did not significantly change the percentage of ferrite sideplates while it progressively reduced the amount of grain boundary ferrite. With a lower manganese level (0.7%), varying the nickel content within the intermediate range (from 2.5 to 3.5%), similarly did not influence the formation of the sideplate structures, but significantly reduced the grain boundary ferrite. Nevertheless, when the nickel content was increased to its highest level, *i.e.*, 5.5%, the volume fraction of both grain boundary ferrite and sideplates was substantially decreased and a considerable amount of martensite was formed (30%). A similar case was observed in the C1 weld. Plotting the quantitative data of Table 3 clearly reveals the trend as illustrated in Fig. 17. It is considered that, because changes in grain size will affect the γ-α transformation behavior (Ref. 17), the latter findings are a result of the combination of the increasing matrix hardenability and the massive increase of the columnar grain size with large nickel additions.

It is well known that nickel is an austenite stabilizer like manganese (Ref. 2). The addition of nickel will increase the matrix hardenability of the weld met-

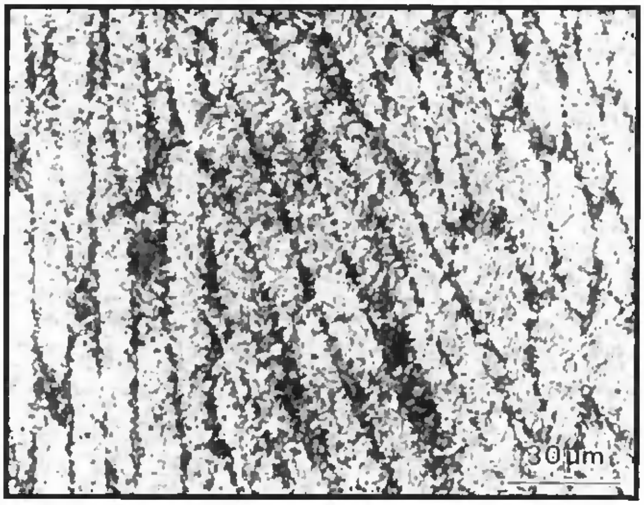

Fig. 11 — The segregation structure in the B3 weld metal.

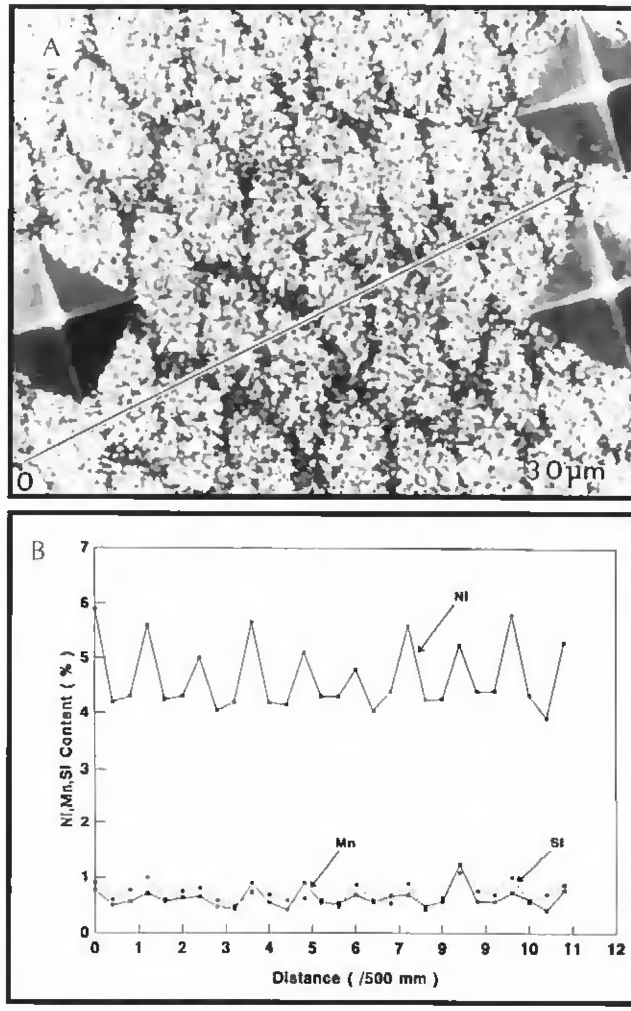

Fig. 12 — Mn, Ni and Si content distribution along the lateral section of the segregation structures in the B3 weld metal. A — The analyzing line and corresponding microstructure; B — EDS results.

als and delay the transformation of ferrite (Refs. 6–9). It should therefore be noted that the level of nickel addition needs to be closely balanced with the manganese content. The microstructures obtained in the A2, B3 and C1 welds indicate that for a given manganese concentration, nickel additions beyond certain limits will result in martensitic structures being promoted. For example, in the B3 weld (manganese content, 0.7%), a nickel content of 5.5% produced 30% martensite. Similarly, Evans (Ref. 5) obtained ~30% martensite in his 1.8% Mn-3.5% Ni low carbon weld metal (carbon level: 0.05%).

In the reheated regions, the effect of nickel was obvious. In the high-temperature reheated regions, the microstructural variation as a result of increasing the nickel content, mentioned in the previous section, was essentially the same as that in the as-deposited weld metals, *i.e.*, grain boundary ferrite formed at the prior γ grain boundaries was progressively replaced by acicular ferrite and even martensite (when the nickel content was sufficiently high). The variation in the amount of sideplates could also be observed but to a lesser extent. In the lower-temperature reheated regions, however, the metallographic observations showed a different situation. The structure with high Mn-medium Ni (*i.e.*, 1.6% Mn, 2.5% Ni) or low Mn-high Ni (*i.e.*, 0.7 or 0.3% Mn, 5.5% Ni) exhibited a distinctive "structure inheritance" feature and the normal changes in grain structure due to recrystallization did not completely remove the preexisting columnar structure. The microstructure produced in these regions consisted mainly of ferrite sideplates, acicular ferrite, martensite and a few grain boundary ferrite rather than the usual well-refined equiaxed ferrite grains. The change was particularly pronounced in the case of the B3 weld (Fig. 8B), where the presence of martensite in the lower-temperature reheated region was obvious. A similar effect was observed by Evans (Ref. 5) in a 1.8% Mn-3.5% Ni low carbon C-Mn weld, although in that case he found the ordinary refined ferrite grains were replaced by sideplate-type colonies.

Considering the corresponding as-deposited microstructures of the A2 and B3 welds in which the low-temperature reheated regions were not refined, it was noted that both these microstructures contained a certain amount of martensite (6% in A2 and 30% in B3). It is considered possible that this martensite existed prior to the reheating procedures and influenced the reaustenitization characteristics of the weld metals at very rapid heating rate conditions of welding and resulted in γ grains with a larger grain size. During the subsequent cooling process, these large austenite grains then generated microstructural constituents that would normally develop from larger γ grains. This "structure inheritance" effect has been previously observed in multi-reheated HAZ region of a quenched-tempered alloy steel (Ref. 18). Evans (Refs. 5, 19, 20) has also reported a similar incomplete refinement in the low-temperature reheated regions of some high hardenability Cr-, Mo- and Ni-bearing C-Mn welds and called it a "memory" effect (Ref. 5). Further investigation, however, is obviously required to clarify the matter in detail. For example, studies of the lower temperature (*e.g.*,

Table 5 — Influence of the Nickel Content on the Formation of Grain Boundary Ferrite and Ferrite Sideplates in the Top Bead (↓ = decrease)

Mn level	Ni level	Effect on PF(G)	Effect on FS(A)
1.6%	1.0%	large ↓	very small↓
	2.5%	large ↓	small ↓
0.7%	2.5%	large ↓	very small ↓
	3.5%	large ↓	very small ↓
	5.5%	large ↓	large ↓
0.3%	5.5%	large ↓	large ↓

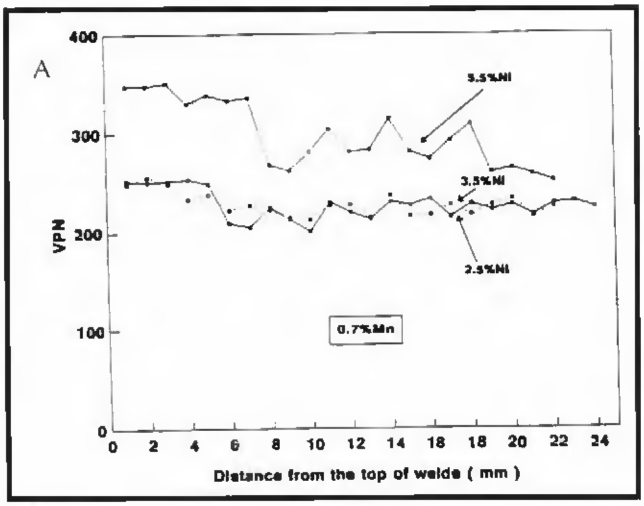

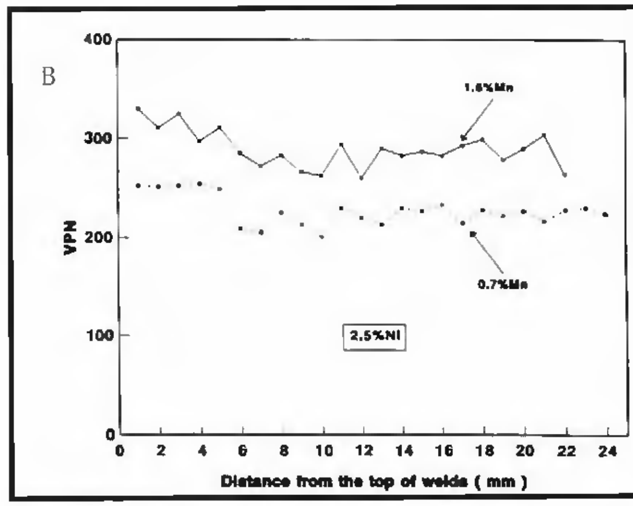

Fig. 13 — *Hardness variations along the through-thickness centerline of the SMA C-Mn-Ni welds showing the effect of nickel on the weld metal hardness. A — Manganese content 1.6%; B — manganese content 0.7%.*

~900°C) continuous reheating transformation behavior (*i.e.*, the α-γ transformation during continuous heating) of the relevant weld metals would be helpful in understanding this effect.

The influence of manganese content on the weld metal microstructure is shown by comparing the microstructures produced in the A1 and B1 or B3 and C1 welds, in which the manganese content was changed from 1.6 to 0.7% or from 0.7 to 0.3% while nickel levels remained constant (*i.e.*, 2.5 or 5.5%). The essential effect of manganese is to promote the acicular ferrite transformation at the expense of both grain boundary ferrite and sideplate structure. If, however, the nickel content is high enough, increasing manganese would result in the formation of martensite, as in the case of the A2 and B3 welds. These coincide with the traditional understanding of the role of manganese (Refs. 6, 7, 21). In addition, it was noted that the quantitative results indicated that manganese exhibited a stronger potential for suppressing grain boundary ferrite and sideplates and encouraging intragranular products than nickel. This follows their capacities to influence the matrix hardenability as described by Grange (Ref. 22). According to Grange (Ref. 22), the effect of manganese was estimated to be about two times that of nickel. The dilatometric studies of the continuous cooling transformation behavior of the weld metals confirmed this hardenability relationship (Refs. 8, 9).

Combining the microstructural data from the current investigation with those reported by Harrison and Farrar (Refs. 6, 7) and Evans (Ref. 5), Fig. 18 illustrates the relationship of the nickel and manganese contents and the volume fraction of acicular ferrite formed in the as-deposited C-Mn-Ni weld metals with carbon levels of 0.04–0.05%. This figure reveals that there is an optimum compositional range of the nickel and manganese contents for a high percentage of acicular ferrite. A combination of the nickel and manganese contents inside this range would produce acicular ferrite of 70–85%, while compositions outside the range would either result in a large amount of proeutectoid ferrite or introduce a high percentage of martensite, both of which could lead to poor toughness.

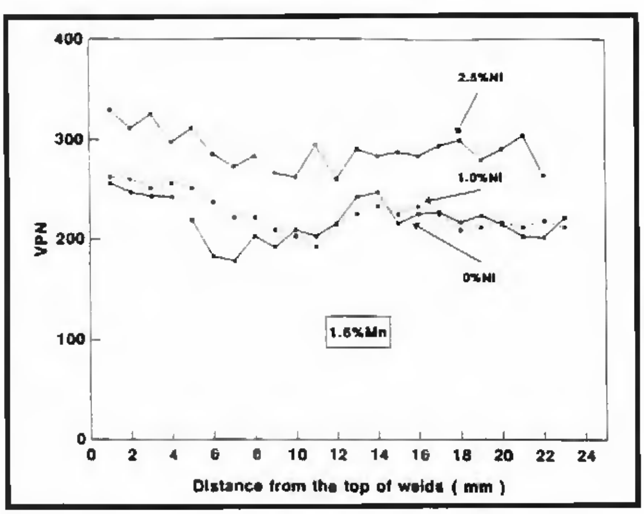

Fig. 14 — *Hardness variations along the through-thickness centerline of the SMA C-Mn-Ni welds showing the effect of manganese on the weld metal hardness.*

It should be particularly noted that martensite will form in the weld metal microstructure when the addition of manganese and nickel is not properly balanced. As shown in Fig. 19, there is a martensite start line (M_s) that lies in the composition region where the highest percentage of acicular ferrite was obtained. This line was determined from detailed optical examination (Ref. 8). In the A2, B3 and C1 weld deposits, the combination of the nickel and manganese contents were beyond the martensite start line. Even though there was a large amount of acicular ferrite in their microstructures in the top bead (*i.e.*, 79% in the A2 weld, 63% in B3 and 67% in C1), there was also some martensite being produced simultaneously in these welds, particularly in high-nickel-content welds (*i.e.*, 30% in the B3 weld and 22% in C1). The as-deposited A1, B1 and B2 welds, on the other hand, possessed a reasonably high percentage of acicular ferrite (*i.e.*, 77% in the A1, 57% in the B1 and 61% in the B2 weld, respectively) but no martensite, because the combination of their nickel and manganese contents were well away from the martensite line. Once martensite is present (and accompanied by other undesirable features, such as segregation structures), the toughness of the weld metals would be seriously impaired. This explains the indications in Figs. 15 and 16 that the optimum toughness values were obtained from the weld metals in which the nickel + manganese content was well away

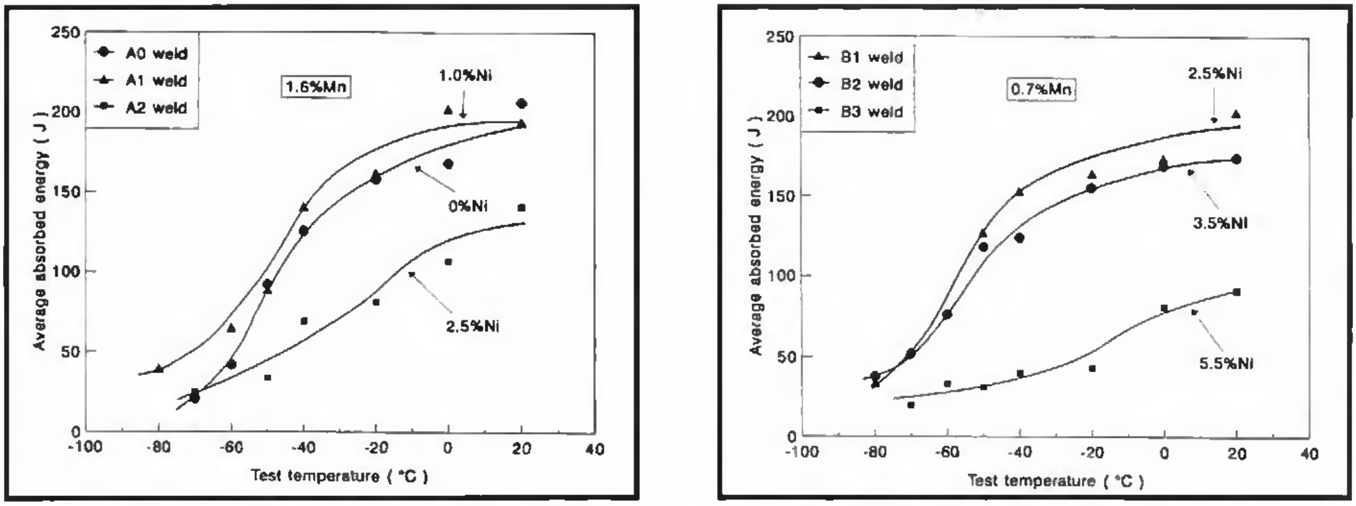

Fig. 15 — Effect of nickel on the Charpy impact curves. A — Manganese content 1.6%; B — manganese content 0.7%.

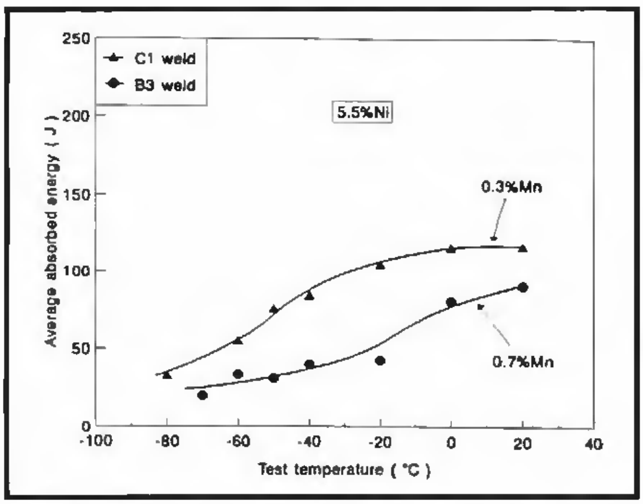

Fig. 16 — Effect of manganese on the Charpy impact curves (5.5% Ni).

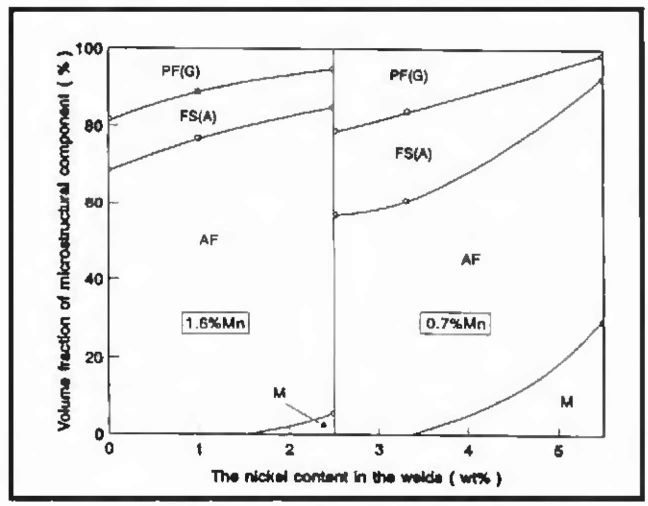

Fig. 17 — Influence of nickel content on weld metal microstructure (PF(G): grain boundary ferrite; FS(A): ferrite sideplates; AF: acicular ferrite; M: Martensite).

from the M_s line and beyond the proeutectoid ferrite-rich area.

Toughness of the C-Mn-Ni Weld Metals and the Effect of Nickel and Manganese

From the data shown in Table 4 and Figs. 15 and 16, it can be seen that at a high manganese level (1.6% Mn), an addition of 1.0% nickel provided the best toughness throughout the range from 20 to –80°C, while a 2.5% Ni content substantially depressed toughness. With a lower manganese level (0.7% Mn), the addition of a medium amount of nickel (2.5–3.5%) displayed satisfactory toughness, and particularly improved the toughness at low temperatures (e.g., at –40°C to ~–60°C). When the nickel content was increased to 5.5%, however, the toughness dropped dramatically. These results can be understood by considering the microstructural variations with the change in chemical composition. For example, in the B3 and C1 welds, the addition of 5.5% Ni resulted in a considerable amount of martensite being introduced into the weld metals, the reheated regions were not refined as usual, a severe segregation structure appeared, and very large columnar grains were obtained. All these would have a deleterious effect on the weld metal toughness. The reasons for the poor performance of the A2 weld were similar to the above but did not depend on the columnar grain size effect.

The effects of columnar grain size and the segregation structures were clearly observed from the SEM examination of the fracture surface of the impact specimens, as shown by Figs. 20–22 (specimens were tested at –50°C). With the B1 weld, the fractures normally went across the columnar grains and were dominated by quasi-cleavage — Fig. 20. In the case of the B3 (or C1) weld, however, most fractures were intercolumnar and linked by both quasi-cleavage and microvoid coalescence (Fig. 21), reflecting the deleterious effect of larger columnar grains on weld metal toughness. In addition, some parallel features were observed on the fracture surface of the B3 and C1 specimens, as illustrated by Fig. 22, and the width of these features matched that of the segregation pattern. Moreover, EDS analyses demonstrated that the fracture surfaces were rich in the main alloying elements, *i.e.*, nickel, manganese and silicon (Ref. 8). These suggest a relationship between the segregation structures and the crack path of the fracture during the impact testing. The morphology changes in acicular ferrite, particularly in the A2, B3 and C1 welds, could also contribute a deleterious effect on the weld metal toughness as has been discussed previously (Ref. 15).

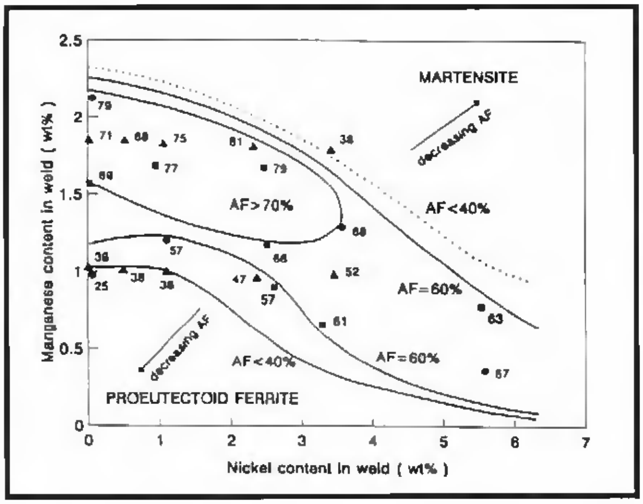

Fig. 18 — Influence of the manganese and nickel contents on the volume fraction of acicular ferrite in weld metal (carbon level: 0.04–0.05%) (■ current results; ● after Harrison and Farrar (Refs. 6, 7); ▲ after Evans (Ref. 5).

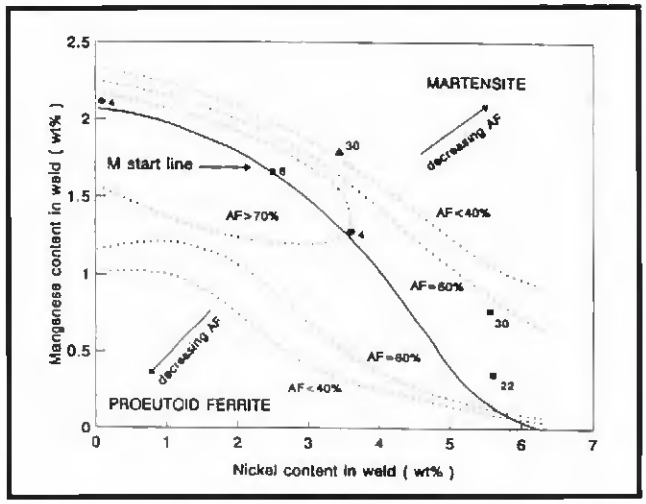

Fig. 19 — Figure 18 with the martensite start line (values are volume fraction of martensite) (■ current results; ● after Harrison and Farrar (Refs. 6, 7); ▲ after Evans (Ref. 5)).

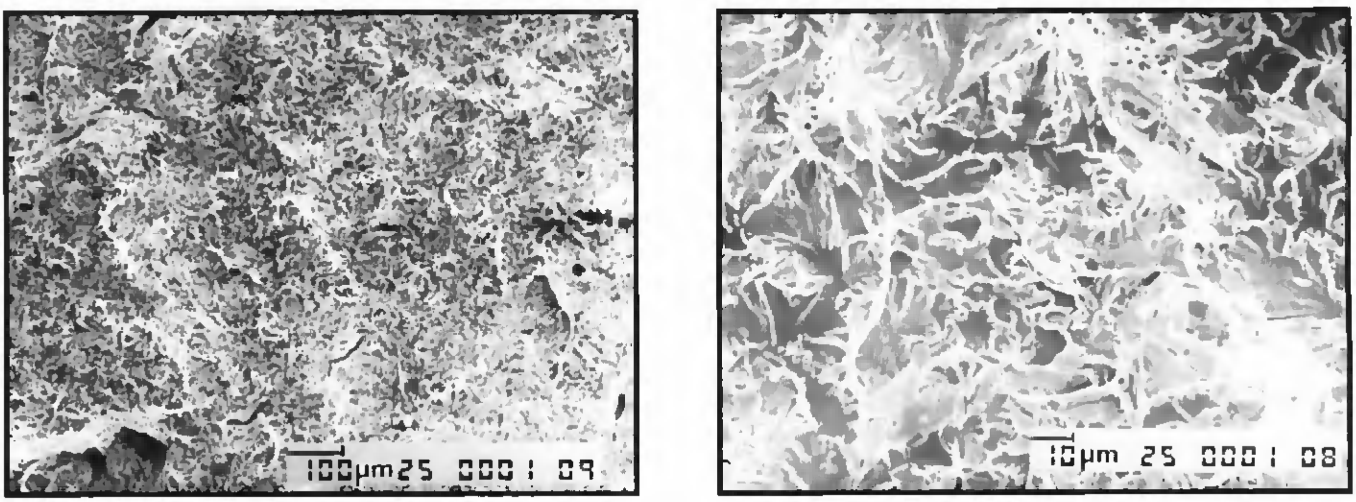

Fig. 20 — Fractograph showing a high density of quasi-cleavage fracture on the B1 weld impact specimen (–50°C).

The toughness results again indicate that the addition of nickel and manganese should be carefully balanced. Different manganese levels require different nickel contents. For the best low-temperature impact toughness (*i.e.*, >120 J at –50°C), the following combinations of the manganese and nickel contents are suggested, *i.e.*, 0.6–1.4% Mn and 1.0–3.7% Ni. This is illustrated by Fig. 23, which shows the relationship between the nickel and manganese contents and weld metal toughness at –50°C. The figure is based on the current studies and data reported by Evans (Ref. 5). If the addition of nickel exceeds these limits, *i.e.*, 2.5% Ni for 1.6% Mn or 5.5% Ni for 0.7% Mn, the properties will be considerably impaired because of the introduction of martensite and a microsegregation effect in the microstructure (Ref. 14) coupled with the additional possibility of coarsened austenite grains.

It is generally believed that 80–90% acicular ferrite content in an as-deposited weld is necessary to obtain satisfactory toughness at low temperatures (e.g. –50 to ~–60°C) (Ref. 23). However, comparing the weld low-temperature toughness variations shown in Fig. 23 with the microstructural changes corresponding to the manganese and nickel contents (Fig. 18), it was noted that the best toughness (*i.e.*, impact energy >120 J at –50°C) was associated with microstructures consisting of 50–75% acicular ferrite with other proeutectoid ferrite components. The microstructures containing higher acicular ferrite (e.g., >75%), on the other hand, did not provide expected properties. This indicates that a finer microstructure may not be always beneficial to weld metal toughness when the deposits are overalloyed, as reported by Munning Schmidt-Van Derr Burg, *et al.* (Ref. 24), and more recently by Svensson and Gretoft (Ref. 23). Sometimes, a simultaneous increase in hardness and strength, and other microstructural changes, such as the presence of segregation structures and/or martensite (as discussed above) could offset the positive effects of fine-grained acicular ferrite, although acicular ferrite might be produced in an increased amount. Therefore, care should be taken when trying to obtain a high proportion of acicular ferrite by increasing alloy contents. In their review, Farrar and Harrison (Ref. 3) have concluded that the best combi-

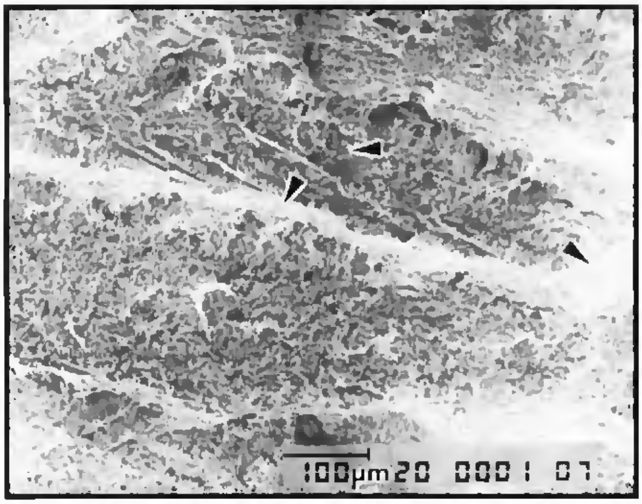

Fig. 21 — Fractograph showing intercolumnar fracture linked by both quasi-cleavage and microvoid coalescence (as indicated by arrows) on the B3 weld impact specimen (–50°C).

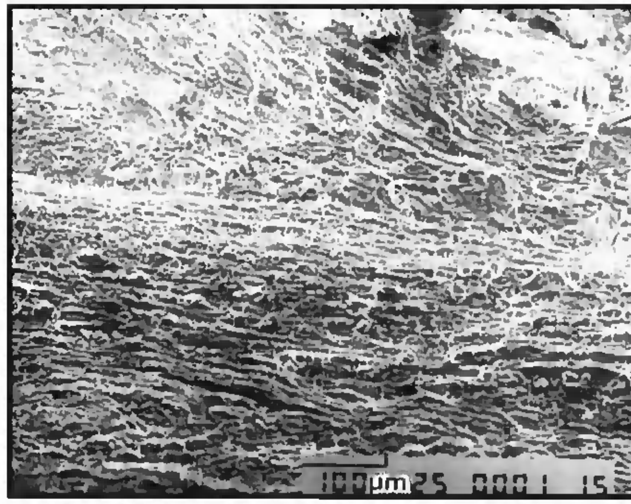

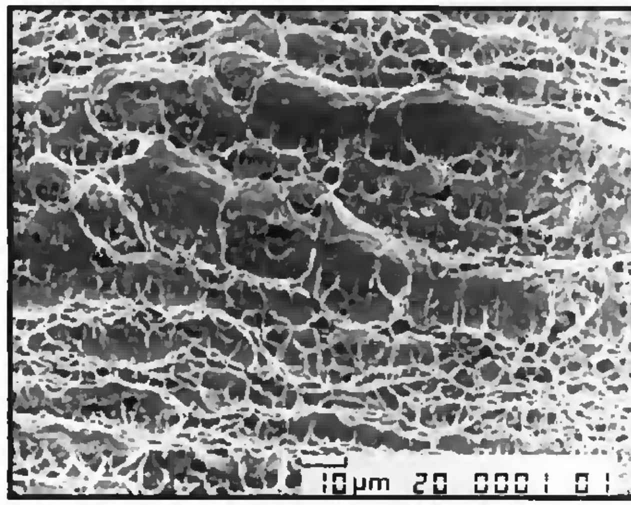

Fig. 22 — Fractograph showing fracture with parallel features on the C1 weld impact specimen (–50°C).

nation of properties of low-alloy weld metals could be obtained when there was more than 65% acicular ferrite. Svensson and Gretoft (Ref. 23) further pointed out the positive effect of only 50% acicular ferrite. This requirement for the optimum acicular ferrite content is consistent with the value range suggested by the results of the current work. It can be concluded that in the alloying practice of low-alloy weld consumables, the essential principle should be an optimum microstructural combination dominated by acicular ferrite rather than merely the highest level of acicular ferrite content, *i.e.*, achieving high enough proportion of acicular ferrite and, at the same time, ensuring the least presence of microsegregation structures and martensite, and without too high matrix hardness and strength.

Nevertheless, it should be noted that for an ideal weld, it is desirable to achieve both excellent low-temperature toughness and adequate yield strength, a combination required for critical industrial structures. To further evaluate the impact results and the effect of nickel and manganese from the point of view of a combination of strength and toughness, the average hardness of the microstructure that was sampled by the notch in the Charpy specimens was measured, and the approximate tensile strength of the area was determined from the Vickers Pyramidal hardness number (VPN), as shown in Table 6.

Considering the impact test results shown in Table 4, together with the tensile strengths (and by implication, the yield strengths) shown in Table 6, it is evident that both the strength and the impact properties are a function of alloying content. The effects of increasing the nickel contents at two distinct levels of manganese, namely 1.6 and 0.7 wt-% (*i.e.*, the weld series A0–A2 and series B1–B3), reveals that as the tensile strength rises in the two series, the Charpy V-notch impact energies (at –50°C) decrease by ~70% in both cases. This suggests that high strength and high toughness weld metals can be achieved at high nickel concentrations only if the manganese level is reduced below 0.7 wt-%.

Conclusions

A systematic study of the microstructure and mechanical properties of the SMA C-Mn-Ni all-deposited weld metals has been carried out, and the following conclusions can be drawn:

1) The microstructure of the C-Mn-Ni weld metals consisted mainly of grain boundary ferrite, ferrite sideplates and fine-grained acicular ferrite, and is dominated by acicular ferrite, the proportions being dependent upon the chemical composition (*e.g.*, manganese and nickel) of the welds.

2) The effect of manganese was to promote acicular ferrite at the expense of proeutectoid ferrite. It was noted that manganese has a stronger potential in suppressing the formation of sideplate

Table 6 — Average Hardness of Microstructure sampled by the Charpy Notch and the Corresponding Tensile Strength of the Same Area

Weld Code	VPN (Load: 10 kg)	Tensile Strength[a] (MPa)
A0	210	675
A1	219	720
A2	281	931
B1	219	720
B2	224	745
B3	298	985
C1	271	904

(a) The tensile strength values were determined using the Vickers hardness numbers according to the *ASM Metals Handbook* (Ref.25).

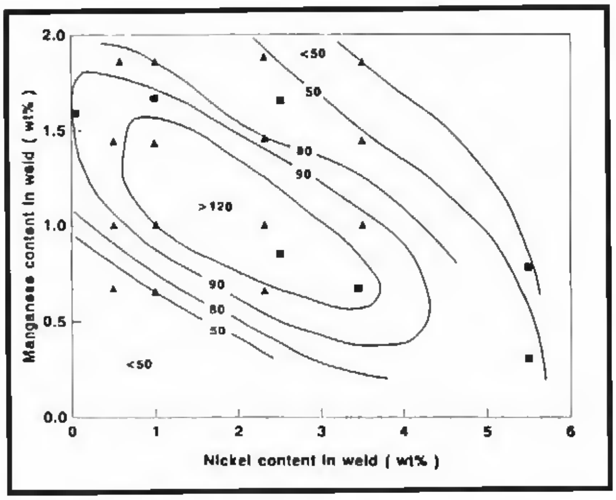

Fig. 23 — Influence of weld metal nickel and manganese contents on Charpy energy (J) at –50°C. (■ current results; ▲ after Evans (Ref. 5).

structures compared to nickel.

3) With increasing nickel content the amount of grain boundary ferrite decreased and acicular ferrite increased as observed with increases in manganese content. At high nickel content, some martensite was formed.

4) Nickel also influences weld microstructure through changing the columnar grain size. The addition of nickel initially refined the prior austenite grain size but further additions caused it to rapidly coarsen.

5) A high nickel content, thus high matrix hardenability, induced a "structure inheritance" effect in the reheated regions that inhibited further refinement. High nickel content also encouraged a "microsegregation" structure that appeared as a martensitic structural banding in the as-deposited weld and hence precipitated a network or parallel morphologies of carbides in the lower-temperature reheated regions.

6) The toughness and hardness of the C-Mn-Ni weld deposits varied according to the alloying contents (*i.e.*, the nickel and manganese concentrations), and resultant weld metal microstructure. An excellent combination of strength and toughness was associated with welds of 1.6%Mn-1.0%Ni and 0.7%Mn-2.5 to ~3.5%Ni. Weld metals with higher nickel contents (*i.e.*, 2.5% for 1.6% Mn level and 5.5% for 0.7–0.3% Mn levels) exhibited poor toughness due to the formation of martensite, the presence of the coarsened columnar grains, a segregation structure and possibly an inherited structure in the reheated regions.

7) A combination of 50–75% acicular ferrite with grain boundary proeutectoid ferrite structures provided the best toughness, whilst a very high proportion of acicular ferrite, but which was associated with other microstructural features, such as martensite and segregation structures, (and hence high matrix hardness/strength) produced poor properties.

Acknowledgments

The authors wish to thank Metrode Products Limited, Chertsey, Surrey, England, for sponsoring the project. Sincere thanks are extended to Dr. J. C. Farrar, Dr. G. S. Barritte and Mr. P. Stubbington for assistance in preparing welds and many helpful discussions during the progress of this work.

References

1. Abson, D. J., and Pargeter, R. J. 1986. *Inter. Metal Rev.*, 31:141–194.

2. Grong, O., and Matlock, D. K. 1986. *Inter. Metal Rev.*, 31: 27–48.

3. Farrar, R. A., and Harrison, P. L. 1987. *J. Mater. Sci.*, 22: pp. 239–244.

4. Taylor, D. S., and Evans, G. M. 1983. *Metal Constr.*, 15: pp. 438–443.

5. Evans, G. M. 1991. *Joining Sciences*, 1: pp. 2–13.

6. Harrison, P. L., and Farrar, R. A. 1987. *Metal Constr.*, 19: pp. 392R–399R and 447R–450R.

7. Harrison, P. L. 1983. Ph.D. thesis, University of Southampton, Southampton, U.K.

8. Zhang, Z. 1994. Ph.D. thesis, University of Southampton, Southampton, U.K.

9. Farrar, R. A., and Zhang, Z. 1993. *Proc. of The 6th International Conference of JOM*, April 4–6, 1993. European Institute of Joining of Materials, Helsingor, Denmark, pp. 397–404.

10. Abson, D. J. 1993. *Welding Journal*, 72(5): 173-s to 187-s.

11. Surian, E. S., Trotti, J. L., and Boniszewski, T. 1992. *Welding Journal*, 71(7): 263-s to 268-s.

12. Pickering, F. B. 1975. Paper presented at conference on Quantitative and Qualitative Metallurgy, Sheffield, U.K., July 17–18, 1975, The Institute of Metallurgical Technicians.

13. Davey, T. G., and Widgery, D. J. 1976. The Welding Institute, Abington, England, DOC. II-A-389-76, 1976.

14. Zhang, Z., and Farrar, R. A. 1995. Columnar grain development in C-Mn-Ni low alloy weld metals and the influence of nickel. *J. Mater. Sci.*, 30: pp. 5581–5588.

15. Farrar, R. A., and Zhang, Z. 1995. Aspect ratios of acicular ferrite in Ni bearing weld metals. *Mat. Sci. Tech.* 11: pp. 759–764.

16. Zhang, Q., and Farrar, R. A. 1994. A study of the precipitation structures in C-Mn-Ni SMA weld metals. Research Report, University of Southampton, Southampton, U.K. ME/94/13.

17. Farrar, R. A., Zhang, Z., Bannister, S. R., and Barritte, G. S., 1993. *J. Mater. Sci.*, 28: pp. 1385–1390.

18. Zhang, Z., and Li, Z., *et al.* 1989. *Proc. of The 4th International Conference of JOM*, March 19–22, 1989. European Institute of Joining and Materials, Helsingor, Denmark, pp. 397–404.

19. Evans, G. M. 1988. *Joining and Materials*, 1: pp. 239s–246s.

20. Evans, G. M. 1989. *Weld. Metal Fabr.*, Aug./Sep., pp. 346-358.

21. Evans, G. M. 1986. *Metal Constr.*, 18: pp. 438R–444R.

22. Grange, R. A. 1973. *Metall. Trans.*, 4: pp. 2231–2244.

23. Svensson, L.-E., and Gretoft, B. 1990. *Welding Journal*, 69(12): 454-s to 461-s.

24. Munning Schmidt-Van Derr Burg, M. A., Hoekstra, S., and Den Ouden, G. 1985. *Welding Journal*, 64(3): 63-s to 70-s.

25. Boyer, H. E., and Gall, T. L. 1984. *ASM Metals Handbook*, Desk Edition, ASM, Materials Park, Ohio.